Thermochimica Acta, 217 (1993) 151–173
Elsevier Science Publishers B.V., Amsterdam

Simulation of dynamical thermogravimetric curves: single and complex reactions

J.J.M. Órfão * and J.L. Figueiredo
Faculty of Engineering, University of Oporto, 4099 Oporto Codex (Portugal)

(Received 27 July 1992)

Abstract

Dynamic thermogravimetry is a technique widely used to study the kinetics of reactions involving solids. In this work, the fundamental properties which determine the shape and position of the TG and DTG curves are defined, namely the kinetic function and two dimensionless parameters $\gamma = E/RT_0$ and $\beta = AT_0/b$. The methodology used is extended to the case of complex reactions (competitive, consecutive and independent), referring to situations which may occur in practice and showing illustrative simulations. The pyrolysis of lignocellulosic materials is taken as an example, using data previously published.

LIST OF SYMBOLS

A	Arrhenius pre-exponential factor
b	heating rate
E	activation energy
k	rate constant
n	reaction order
R	gas constant
s	shape index
T	temperature
T_i	onset temperature ($\alpha = 0.001$)
T_m	temperature at maximum rate
T_0	starting temperature
t	time
W	mass of solid
W_0	initial mass of solid
W_∞	mass of solid residue ($\alpha = 1$)
X	conversion
x	extension variable of the first of two consecutive reactions

* Corresponding author.

y_0 initial mass fraction in a residue free basis
z variable related with α

Greek letters

α Fractional decomposition or degree of transformation
β dimensionless parameter AT_0/b
γ dimensionless parameter (E/RT_0)
θ normalized temperature
θ_1 normalized temperature for $\alpha = 0.001$
θ_m normalized temperature at maximum rate
θ_∞ normalized temperature for $\alpha = 1$
μ stoichiometric parameter in consecutive reactions

INTRODUCTION

Thermogravimetry (TG) is a convenient technique for studying the kinetics of many reactions involving solids, by following the change in mass, or the rate of mass loss (DTG), of the samples with time (or temperature).

Examples of simple reactions of this type are the decomposition of solids such as

(A) Solid 1 → Solid 2 + Gases (e.g. $CaCO_3(s) \rightarrow CaO(s) + CO_2(g)$)
(B) Solid → Gases (e.g. $NH_4NO_3(s) \rightarrow N_2O(g) + 2H_2O(g)$)

and gas–solid reactions such as

(C) Solid + Gas 1 → Gas 2 (e.g. $C(s) + O_2(g) \rightarrow CO_2(g)$)
(D) Solid 1 + Gas 1 → Solid 2 + Gas 2 (e.g. $FeO(s) + H_2(g) \rightarrow Fe(s) + H_2O(g)$)

There are two alternative experimental methods, as follows.

Isothermal TG

The solid reactant is kept under isothermal conditions. Several experiments must be carried out at different temperatures in order to determine the temperature dependency of the reaction rate. In actual practice, a finite time is needed to heat the material up to the desired temperature, so that the initial stages of the reaction occur under non-isothermal conditions. If very high heating rates are used in this period, a non-uniform temperature distribution may result within the solid, and the process becomes uncontrollable [1].

Dynamic TG

The solid sample is submitted to a gradual increase in temperature (usually linear with time). In this case it is possible, in principle, to

determine the kinetic parameters with a single experiment, although the mathematical treatment of experimental data is more complex.

One of the problems associated with this last method is that the kinetic parameters obtained thereof are frequently dependent upon the experimental conditions, such as heating rate, initial amount of solid material, gas phase composition, geometry of the reactor and particle size of the solid [2–8]. Therefore, it is not surprising that quite different values are reported in the literature for the same reaction, as is exemplified by the decomposition of $CaCO_3$ [4].

However, this situation is not a characteristic of dynamic TG. Thus, in recent studies on the decomposition of calcium oxalate monohydrate, the same dependency between the activation energy and the initial amount of solid was determined by either of the two methods [5, 9, 10].

One of the reasons for such experimental observations is certainly related to the complexity of the reaction mechanisms in the solid state and the lack of mechanistic equations accounting in full for the process involved. Moreover, the influence of the gas phase and the problems associated with mass and heat transfer limitations are frequently overlooked [1, 3, 4, 6–8, 11].

Nevertheless, non-isothermal TG continues to be extensively used, given its great experimental simplicity.

In addition, when studying the thermal decomposition of complex materials such as wood or coal, the occurrence of several independent and/or competitive reactions restricts the applicability of the isothermal method, because it is not possible to control the reactions which are initiated before the desired temperature is reached in each experiment.

In the following sections, the dimensionless parameters which govern the shape and position of the non-isothermal TG and DTG curves for single reactions are defined, and their influence upon various observable quantities is studied. The simulations are then extended to complex reactions (competitive, consecutive and independent).

SINGLE REACTIONS

In the decomposition of solids, the rate of reaction depends upon the temperature and amount of substance. Usually it is assumed that these functions are separable, and the equation generally used to describe the progress of reaction is

$$\frac{d\alpha}{dt} = k(T)f(\alpha) \tag{1}$$

where t is the time, T the absolute temperature and α the degree of

transformation or fractional decomposition defined as

$$\alpha = \frac{W_0 - W}{W_0 - W_\infty} \tag{2}$$

where W is the mass of solid and the subscripts 0 and ∞ refer to the starting and end of the reaction.

The temperature dependency is normally expressed by the Arrhenius equation

$$k = A \exp\left(-\frac{E}{RT}\right) \tag{3}$$

where E is the activation energy, A the pre-exponential factor and R the ideal gas constant. Therefore

$$\frac{d\alpha}{dt} = A \exp\left(-\frac{E}{RT}\right) f(\alpha) \tag{4}$$

where $f(\alpha)$ is a function depending upon the reaction mechanism. Some of the most used functions are listed elsewhere [12]. However, some authors prefer to use an empirical kinetic law of the type $f(\alpha) = (1 - \alpha)^n$, where n is a reaction order.

Equation (4) implies additionally that the solid is homogeneous and that internal and external heat transfer resistances are absent. Under certain circumstances, it may be extended to gas–solid reactions. In effect, if these show a reaction order with respect to the gaseous reactant

$$\frac{d\alpha}{dt} = A \exp\left(-\frac{E}{RT}\right) f(\alpha) P_{gas}^{n} \tag{5}$$

If the gas partial pressure P_{gas} does not change significantly in the course of the experiments (which is valid for low gas conversions), then it may be considered constant and included in the pre-exponential factor.

When the reaction is carried out under a linear temperature programme ($T = T_0 + bt$, where b is the heating rate and T_0 the starting temperature), eqn. (4) may be written as

$$\frac{d\alpha}{dT} = \frac{A}{b} \exp\left(-\frac{E}{RT}\right) f(\alpha) \tag{6}$$

Equation (6) may be rendered dimensionless by normalizing the temperatures by the starting temperature and defining a new variable $\theta = T/T_0$, so

$$\frac{d\alpha}{d\theta} = \beta \exp\left(-\frac{\gamma}{\theta}\right) f(\alpha) \tag{7}$$

where $\beta = AT_0/b$ and $\gamma = E/RT_0$.

Considering the simplifications introduced, the non-isothermal TG and

DTG curves depend only on these two dimensionless parameters and on the kinetic function.

The first parameter is the ratio between a time constant for heating (T_0/b) and a time constant for reaction ($1/A$). The second parameter includes the activation energy for the reaction, and is referred to as the Arrhenius parameter. It should be noted that the procedural variables heating rate and initial temperature affect β and γ. When b increases β decreases and when T_0 increases β also increases, but γ decreases.

Results

Equation (7) was integrated by the 4th order Runge–Kutta method with a variable integration step, for values of γ between 10 and 90 and β between 10 and 10^{10}. A large number of real cases is included within such ranges. The kinetic functions considered were those of the type $f(\alpha) = (1-\alpha)^n$, with $n = 0, 1/2, 2/3, 1, 3/2$ and 2 and also some mechanistic expressions, namely

$$f(\alpha) = \frac{(1-\alpha)^{2/3}}{1-(1-\alpha)^{1/3}} \qquad \text{(Mechanism D3)}$$

$$f(\alpha) = [-\ln(1-\alpha)]^a(1-\alpha), \quad \text{with } a = 1/2 \text{ and } 2/3 \qquad \text{(Mechanisms A2 and A3)}$$

The symbology used for these mechanisms is the usual one [12].

The initial condition is: for $\theta = 1$ (or $T = T_0$), $\alpha = 0$. When applying the method to the mechanistic functions considered, there is a numerical problem, because for $\alpha = 0$, $f(\alpha) \rightarrow \infty$ in the first case, and $f(\alpha) = 0$ in the second. A change in variable may be used to circumvent this problem, transforming eqn. (7) into another of the form

$$\frac{dz}{d\theta} = \beta \exp\left(-\frac{\gamma}{\theta}\right) \tag{8}$$

Therefore, the relationship between z and α must be obtained by solving the equation

$$dz = \frac{1}{f(\alpha)} d\alpha \tag{9}$$

The results are:

Mechanism D3 $$z = -3(1-\alpha)^{1/3} + \frac{3}{2}(1-\alpha)^{2/3} \tag{10}$$

Mechanism A2 $$z = 2[-\ln(1-\alpha)]^{1/2} \tag{11}$$

Mechanism A3 $$z = 3[-\ln(1-\alpha)]^{1/3} \tag{12}$$

where the variable takes an initial value of $-3/2$ for the first mechanism and of zero for the others.

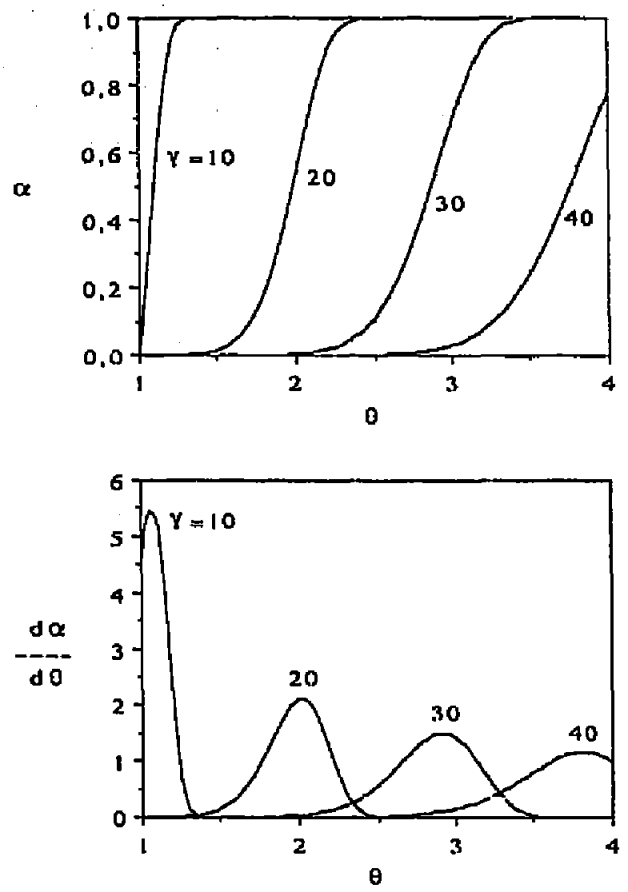

Fig. 1. TG and DTG curves for $n = 1$, $\beta = 10^5$ and various values of γ.

Figure 1 shows the influence of the Arrhenius parameter for a first order reaction with $\beta = 10^5$. When γ increases, the peaks broaden and are displaced towards higher temperatures, while the maximum rate decreases. Because $\gamma = E/RT_0$, this last observation is a direct result of the well-known fact that reactivities decrease when the activation energy increases. Similar DTG curves (in terms of changes in volume of gaseous products released versus time) were reported by Jüntgen and van Heek [13].

Figure 2 shows the effect of β on the shape and position of TG and DTG curves for the kinetic function $f(\alpha) = (1 - \alpha)$ and for $\gamma = 20$. It may be observed that a decrease in β has a similar effect to an increase in γ, namely a decrease in reactivity. Because β is inversely proportional to the heating rate, the normalized curves show the great influence of this procedural variable, even when the heat transfer resistances between the heating element and the interior of the solid sample is disregarded [3].

Figure 3 shows the normalized TG and DTG curves simulated with $\gamma = 20$, $\beta = 10^5$ and various values of the reaction order n.

When the reaction order increases, the maximum rates decrease, as do the temperatures at which these maxima occur θ_m, although this last effect is not very significant (as shown in Table 1). However, it is interesting to

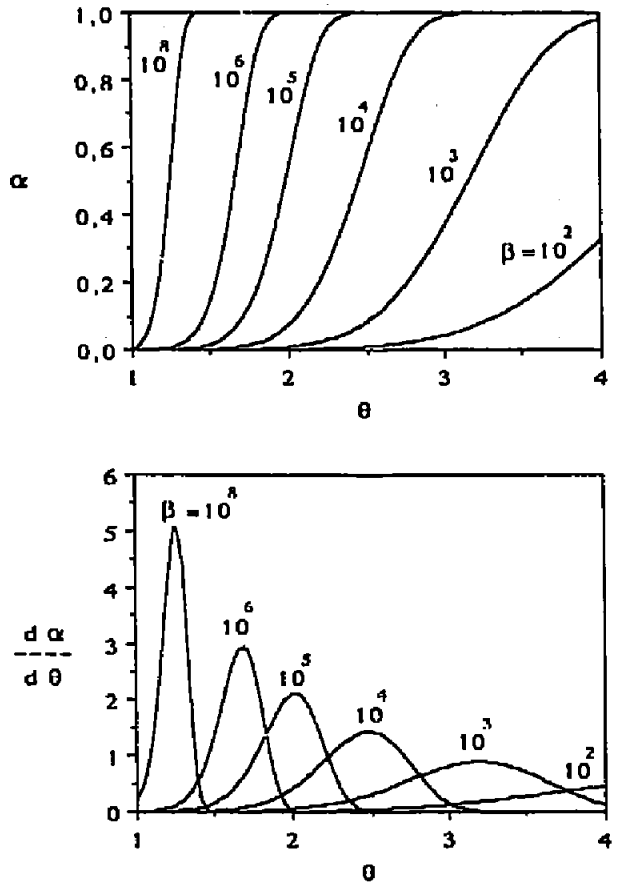

Fig. 2. TG and DTG curves for $n = 1$, $\gamma = 20$ and various values of β.

note that the reaction begins at practically the same temperature, independently of n.

If a shape index s is defined in the usual manner as the ratio of the derivatives of the DTG curve at the inflexion points to the left and right of the maximum [14], it may be observed that it increases gradually with reaction order, the higher symmetry being obtained for $n = 3/2$ (see Table 1).

Finally, Fig. 4 shows the simulated results for mechanisms D3, A2 and A3, for $\gamma = 20$ and $\beta = 10^5$. In the first case, comparing with the pseudo-homogeneous kinetic laws, it may be observed that the maximum rate is similar to that of reaction order 3/2, but the reactivity is much higher, because the reaction occurs at much lower temperatures. The mechanistic functions A2 and A3 lead to sharp peaks and the maxima are higher, although the reaction starts at higher temperatures. The shape index lies between 0.5 and 0.6 for these three rate laws.

Relationship between peak position and the parameters γ *and* β

The normalized temperatures θ_m at which the maxima occur, may be plotted versus γ and β, as shown in Fig. 5. This shows a linear dependency

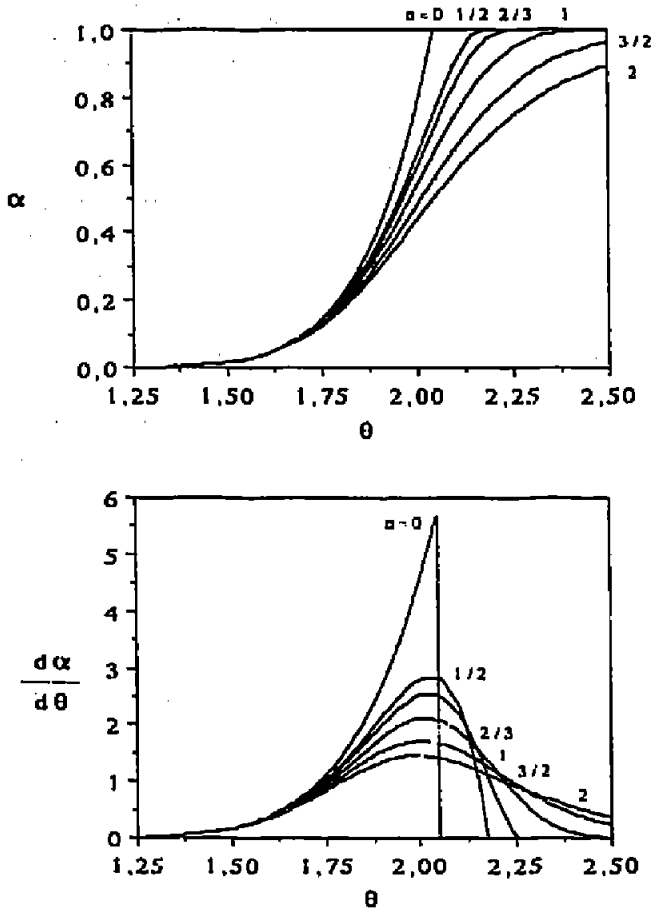

Fig. 3. Influence of the reaction order for kinetic laws of the type $f(\alpha) = (1 - \alpha)^n$ on the TG and DTG curves with $\gamma = 20$ and $\beta = 10^5$.

except when γ is low and β is high simultaneously. In this case, there are no peaks in the DTG curves, but rather a gradual decrease in rate, so that θ_m is very close to 1. Although Fig. 5 refers to the kinetic law $f(\alpha) = (1 - \alpha)$, the same behaviour is found for all other kinetic functions considered, including the mechanistic ones.

Similar behaviour is found for other normalized temperatures at fixed

TABLE 1

Features of the DTG curves for $\gamma = 20$, $\beta = 10^5$ and various reaction orders

Feature	n					
	0	1/2	2/3	1	3/2	2
$(d\alpha/d\theta)_m$	5.68	2.86	2.55	2.12	1.72	1.46
θ_m	2.046	2.030	2.026	2.016	2.003	1.992
s	0	0.19	0.39	0.73	1.06	1.29

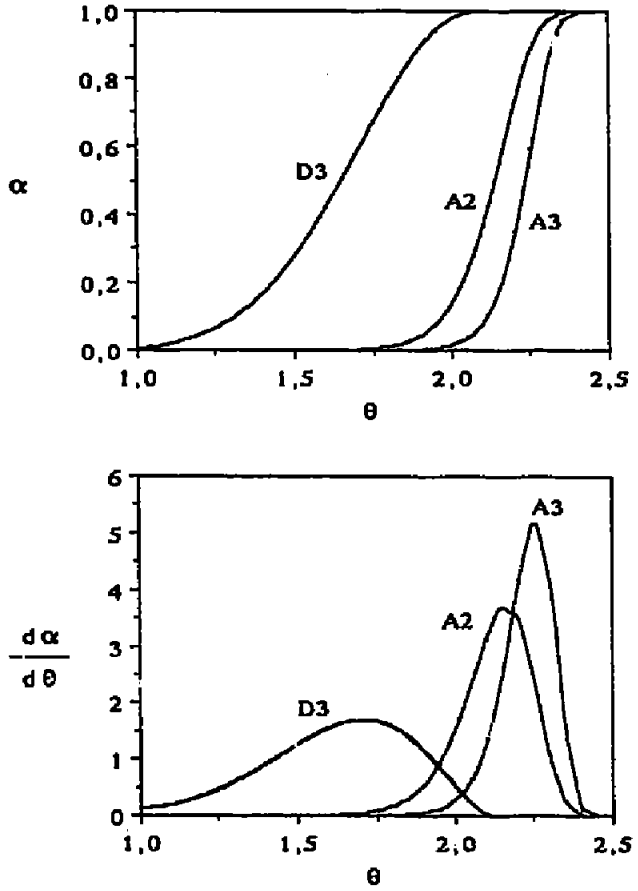

Fig. 4. TG and DTG curves for the mechanistic kinetic functions D3, A2 and A3, with $\gamma = 20$ and $\beta = 10^5$.

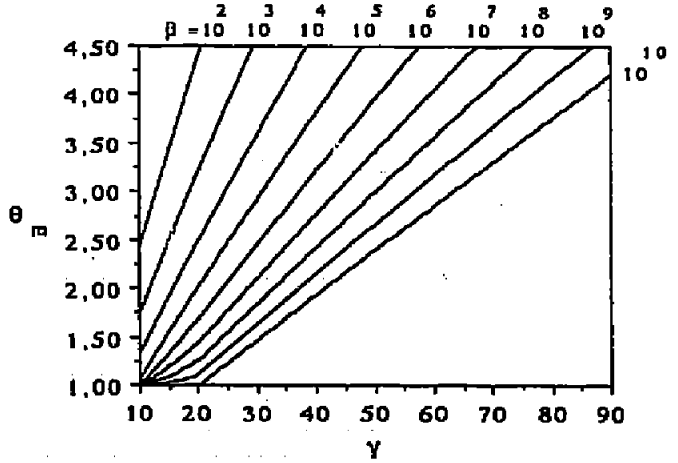

Fig. 5. Position of the peak maxima as a function of γ and β for first order reactions.

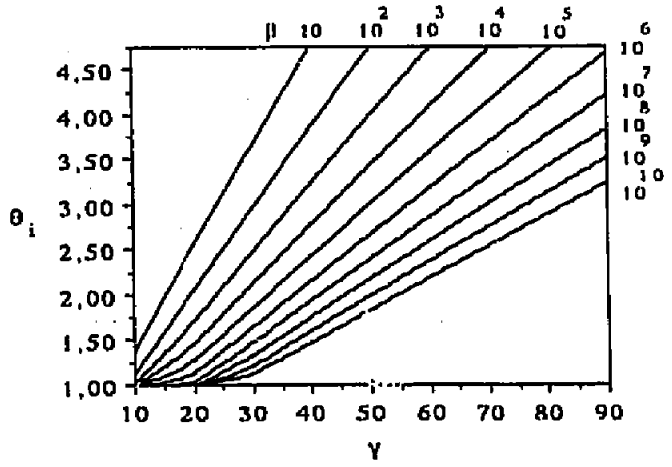

Fig. 6. Dependency of θ_i (normalized temperature for $\alpha = 0.001$) on γ and β for first order reactions.

degree of transformation, such as is shown in Fig. 6 for $\theta_i = T_i/T_0$, where T_i is the onset temperature of the reaction (the threshold being defined for $\alpha = 0.001$). Obviously, the range of values (γ, β) for which $\theta_i \approx 1$ is larger than the corresponding range referred to θ_m.

Influence of the starting temperature and heating rate on the position of the peaks

The dimensionless parameters γ and β depend on the heating rate (β) and the temperature at which the program starts (both). The latter may be different from room temperature. For instance, when the solid is produced *in situ* at a temperature lower than the range at which it reacts, it may be more convenient to start the thermogram at the temperature of production of the solid [15–17].

Table 2 shows some examples of the influence of b and T_0 on the position of the peaks (represented by T_i and T_m, the temperatures corresponding to $\alpha = 0.001$ and the maximum rate, respectively).

By increasing the starting temperature of the thermogram, the peaks are shifted to higher temperatures, this effect being most significant for low values of γ, i.e. for reactions with a low activation energy ($E < 20$ kcal mol^{-1}).

A similar shift in the DTG curves is caused by an increase in the heating rate, as is well-known [18]. However, in this case the effect is more important when the activation energies are high and the pre-exponential factors A in the Arrhenius equation are small (see Table 2), i.e. the effect of

TABLE 2

Influence of the procedural variables b and T_0 on the position of the peaks for first order reactions

T_0 (K)	b (K s^{-1})	γ	β	θ_i	θ_m	T_i (K)	T_m (K)
300	1.0	20	10^3	1.70	3.20	510	960
300	0.1	20	10^4	1.46	2.49	438	747
600	1.0	10	2×10^3	1.02	1.67	612	1002
300	1.0	20	10^5	1.27	2.02	381	606
300	0.1	20	10^6	1.13	1.69	339	507
600	1.0	10	2×10^5	1.00	1.06	600	636
300	1.0	20	10^7	1.03	1.44	309	432
300	0.1	20	10^8	1.00	1.26	300	378
600	1.0	10	2×10^7	1.00	1.00	600	600
300	1.0	50	10^6	2.68	3.95	804	1185
300	0.1	50	10^7	2.41	3.41	723	1023
600	1.0	25	2×10^6	1.36	2.02	816	1212
300	1.0	70	10^9	2.76	3.67	828	1101
300	0.1	70	10^{10}	2.55	3.31	765	993
600	1.0	35	2×10^9	1.39	1.86	834	1116

the heating rate is particularly noticeable when the reactivity of the solid is low. If the heat transfer resistances were included in this analysis, larger shifts would be observed when changing the heating rate [3].

In summary, the starting temperature and the heating rate, among other procedural variables, have been shown to affect the TG and DTG curves, making comparisons between different studies difficult, unless they are performed under exactly the same experimental conditions.

COMPETITIVE REACTIONS

Let us suppose that a solid reactant is converted by two competitive reactions. Because the global rate is the sum of the rates of the two reactions, the appropriate equation is

$$\frac{d\alpha}{d\theta} = \beta_1 \exp\left(-\frac{\gamma_1}{\theta}\right) f_1(\alpha) + \beta_2 \exp\left(-\frac{\gamma_2}{\theta}\right) f_2(\alpha) \qquad (13)$$

Equation (13) may be simplified when both reactions have the same kinetics and the same Arrhenius parameter ($f_1(\alpha) = f_2(\alpha) = f(\alpha)$ and

$\gamma_1 = \gamma_2 = \gamma$). Then

$$\frac{d\alpha}{d\theta} = (\beta_1 + \beta_2) \exp\left(-\frac{\gamma}{\theta}\right) f(\alpha) \quad (14)$$

i.e. we have the same situation as for a single reaction with $\beta = \beta_1 + \beta_2$. In practical terms, this means that when the activation energies are close, it is not possible to obtain individual peaks in the DTG curve, even by changing the operating conditions used, such as the heating rate [19].

Equation (13) was integrated with the initial condition $\theta = 1$ and $\alpha = 0$ for a large range of values of the parameters, and considering kinetic laws of zeroth and first orders for both reactions. Table 3 summarizes the most important characteristics of these reactions; θ_∞ is the normalized temperature for which $\alpha = 1$. For zeroth order reactions, $\theta_\infty = \theta_m$.

When the two reactions in parallel occur in non-intersecting ranges of temperature, the global process follows the kinetics of the lower temperature reaction. Therefore, whenever $\theta_{\infty,1} < \theta_{i,2}$ the transformation is governed by the first reaction. The same situation may be observed even when this condition is not entirely fulfilled, for instance if $\gamma_1 = 20$, $\beta_1 = 10^7$, $\gamma_2 = 10$ and $\beta_2 = 10^2$.

A considerable modification of the kinetic characteristics of the process by introducing a slower competitive reaction is illustrated in Fig. 7, which shows the DTG curves for a system with $\gamma_1 = 10$, $\beta_1 = 10^2$, $\gamma_2 = 20$ and $\beta_2 = 10^3$, considering the four possible combinations of reaction order (0 or 1), and the corresponding curves for each of the single reactions. The most relevant features of the system are summarized in Table 4, which may be compared with the results presented for single reactions in Table 3.

TABLE 3

Features of the single reactions considered in the simulation of complex reactions

γ	β	θ_i	n				
			0		1		
			$\theta_m = \theta_\infty$	$(d\alpha/d\theta)_m$	θ_m	$(d\alpha/d\theta)_m$	θ_∞
10	10^2	1.12	2.60	2.14	2.44	0.83	3.96
20	10^3	1.70	3.31	2.37	3.20	0.90	4.24
20	10^7	1.03	1.46	10.75	1.44	3.98	1.67
30	10^7	1.48	2.13	7.54	2.11	2.78	2.43
30	10^9	1.22	1.65	12.22	1.64	4.52	1.82
40	10^5	2.44	3.86	3.16	3.81	1.18	4.47
40	10^6	2.16	3.24	4.38	3.21	1.63	3.78
70	$10^{7.3}$	2.55	3.32	6.93	3.31	2.56	3.64
80	10^{10}	2.90	3.77	6.13	3.76	2.26	4.17

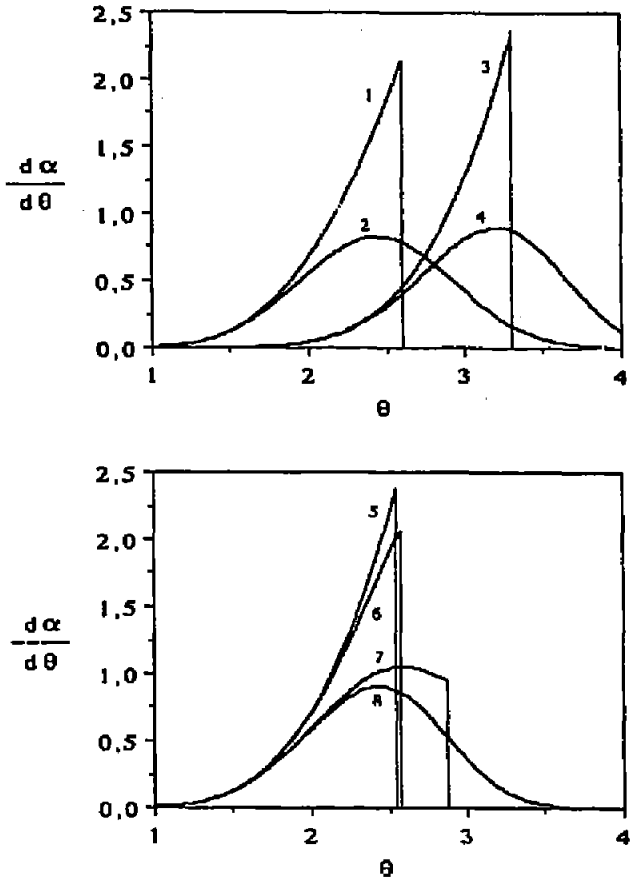

Fig. 7. DTG curves for two reactions in parallel with $\gamma_1 = 10$, $\beta_1 = 10^2$, $\gamma_2 = 20$, $\beta_2 = 10^3$: Upper, single reactions (1, $n_1 = 0$; 2 $n_1 = 1$; 3, $n_2 = 0$; 4, $n_2 = 1$); Lower, reactions in parallel (5, 1 + 3; 6, 1 + 4; 7, 2 + 3; 8, 2 + 4).

The initial stages are governed by the first reaction. It follows that $\theta_i = 1.12$ (cf. Table 3) and the curves for $n_1 = 0$ or $n_1 = 1$ become practically the same, independently of n_2, until a value of θ just above 2. At higher values of θ, the second reaction begins to influence the behaviour of the system, and the global process shows a higher reactivity than that of the first reaction. Such an increase in the rate brings about a decrease in the temperature at which the solid reactant is spent. In the example under

TABLE 4

Features of the system of two competitive reactions ($\gamma_1 = 10$, $\beta_1 = 10^2$, $\gamma_2 = 20$ and $\beta_2 = 10^3$)

n_1	n_2	θ_i	θ_m	$(d\alpha/d\theta)_m$	θ_∞
0	0	1.12	2.55	2.38	2.55
0	1	1.12	2.58	2.07	2.58
1	0	1.12	2.60	1.05	2.88
1	1	1.12	2.44	0.90	3.66

consideration, this is particularly noticeable for $n_1 = 1$ and $n_2 = 0$, where $\theta_\infty = 2.88$ (27% lower than the first reaction alone).

CONSECUTIVE REACTIONS

Let us now assume that the solid reactant produces a gas and a solid intermediate, which also decomposes into gaseous products. Therefore, there are two consecutive reactions from which there is no solid residue ($W_\infty = 0$)

$$\begin{array}{l} \text{S(solid)} \xrightarrow{1} \text{I(solid)} + \text{Gases} \\ \qquad\qquad\quad {\scriptstyle 2}\downarrow \\ \qquad\qquad\quad \text{Gases} \end{array}$$

Kinetic schemes including reactions in series have been proposed, for instance, for the thermal degradation of cellulose [20, 21] and lignin [22].

The fractional decomposition is therefore

$$\alpha = 1 - \frac{W}{W_0} \tag{15}$$

where $W = W_S + W_I$ is the total mass of the sample. The variable defining the extent of the first reaction may be

$$x = 1 - \frac{W_S}{W_{S_0}} = 1 - \frac{W_S}{W_0} \tag{16}$$

Therefore

$$W = W_0(1 - \alpha) \tag{17}$$

$$W_S = W_0(1 - x) \tag{18}$$

$$W_I = W_0(x - \alpha) \tag{19}$$

Let $\mu \in]0, 1[$ be the mass of I produced per unit of S transformed (i.e. μ can take all values between 0 and 1, except 0 and 1). The material balance for S may be written as

$$-\frac{dW_S}{dt} = k'_1 f'_1(W_S) \tag{20}$$

or

$$\frac{dx}{dt} = k_1 f_1(x) \tag{21}$$

However, from the material balance for I

$$\frac{dW_I}{dt} = \mu k'_1 f'_1(W_S) - k'_2 f'_2(W_I) \tag{22}$$

The rate of mass loss is

$$-\frac{dW}{dt} = -\frac{dW_S}{dt} - \frac{dW_I}{dt} = (1-\mu)k_1' f_1'(W_S) + k_2' f_2'(W_I) \tag{23}$$

yielding

$$\frac{d\alpha}{dt} = (1-\mu)k_1 f_1(x) + k_2 f_2(x-\alpha) \tag{24}$$

Considering that the rate constants obey the Arrhenius law and that the temperature is linearly changing with time, eqns. (21) and (24) lead to, respectively

$$\frac{dx}{d\theta} = \beta_1 \exp\left(-\frac{\gamma_1}{\theta}\right) f_1(x) \tag{25}$$

and

$$\frac{d\alpha}{d\theta} = (1-\mu)\beta_1 \exp\left(-\frac{\gamma_1}{\theta}\right) f_1(x) + \beta_2 \exp\left(-\frac{\gamma_2}{\theta}\right) f_2(x-\alpha) \tag{26}$$

By solving this system of differential equations with initial conditions $\theta = 1$ and $x = \alpha = 0$, the behaviour of the system may be simulated under dynamic thermogravimetric conditions. The shape of the curves obtained depends, in addition to the kinetic functions considered, on four kinetic parameters (β_1, γ_1, β_2, γ_2) and one stoichiometric parameter (μ).

Obviously, when the reactivity of the second reaction is much higher than the first, the intermediate I is instantaneously decomposed as it is being formed, so that $W_I \approx 0$ or $\alpha \approx x$. Therefore, the TG and DTG curves become practically the same as those of the first reaction, independently of μ.

If the first reaction begins at a lower temperature than the second, three different situations may be observed, depending on the relative reactivities, as shown in Figs. 8, 9 and 10.

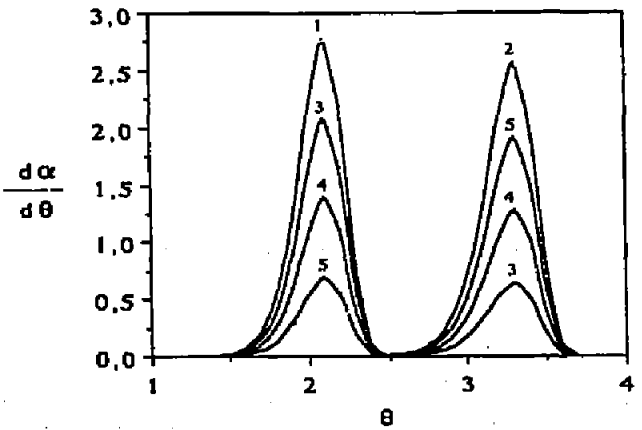

Fig. 8. DTG curves: two single reactions (1, $n_1 = 1$, $\gamma_1 = 30$, $\beta_1 = 10^7$; 2, $n_2 = 1$, $\gamma_2 = 70$, $\beta_2 = 10^{10}$); same reactions in series (3, $\mu = 0.25$; 4, $\mu = 0.50$; 5, $\mu = 0.75$).

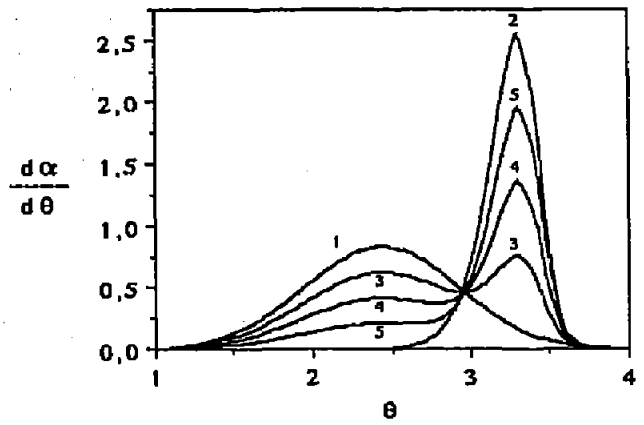

Fig. 9. DTG curves: two single reactions (1, $n_1 = 1$, $\gamma_1 = 10$, $\beta_1 = 10^2$; 2, $n_2 = 1$, $\gamma_2 = 70$, $\beta_2 = 10^{10}$); same reactions in series (3, $\mu = 0.25$; 4, $\mu = 0.50$; 5, $\mu = 0.75$).

In the first instance (Fig. 8) the temperature domains of the two reactions are completely separated (cf. Table 3). Therefore, there are two well resolved peaks, the first corresponding to the formation of I and the second to its decomposition.

In Fig. 9 there are also two peaks (not completely resolved now), although the first may not be well defined for high values of μ. The curves describe the transformation S→I until $\theta = 2.55$ (cf. Table 3) and from there on the joint effect of the two consecutive reactions.

When the two reactions overlap extensively in the temperature domain and the rates are of the same order of magnitude, only one peak may appear in the DTG curve, as illustrated in Fig. 10. In this case, the position of the maximum rate θ_m depends strongly on the parameter μ, and becomes quite distinct from the position of the peaks of any of the two separate reactions for values of μ in the range 0.25–0.50. This illustrates the danger of interpreting thermograms of complex reactions of this type as if they were simple reactions.

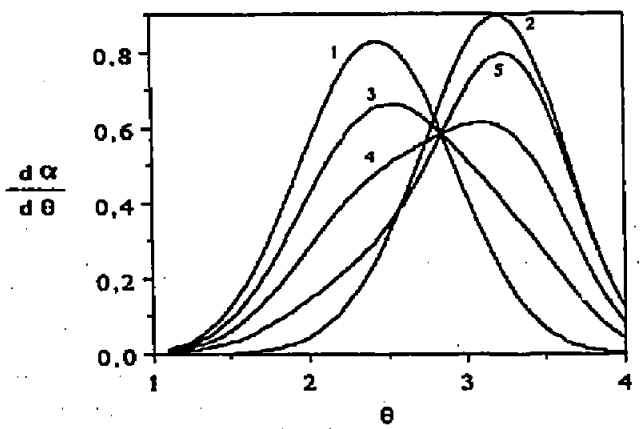

Fig. 10. DTG curves: two single reactions (1, $n_1 = 1$, $\gamma_1 = 10$, $\beta_1 = 10^2$; 2, $n_2 = 1$, $\gamma_2 = 20$, $\beta_2 = 10^3$); same reactions in series (3, $\mu = 0.25$; 4, $\mu = 0.50$; 5, $\mu = 0.75$).

INDEPENDENT REACTIONS

Let us assume that the solid material is made up of m components capable of independent decomposition

$S_1 \rightarrow$ Gas

$S_j \rightarrow$ Gas

$S_m \rightarrow$ Gas

For each of the reactions, a differential equation may be written as

$$\frac{d\alpha_j}{d\theta} = \beta_j \exp\left(-\frac{\gamma_j}{\theta}\right) f_j(\alpha_j) \tag{27}$$

with initial condition $\theta = 1$, $\alpha_j = 0$ and

$$\alpha_j = \frac{W_{j0} - W_j}{W_{j0}} = X_j \tag{28}$$

i.e. the fractional decomposition of each component is equal to the respective conversion X_j because the residue (if present) is assumed to result from non-reactive components present in the solid, with total mass W_∞.

Therefore

$$W_j = W_{j0} - W_{j0}\alpha_j \tag{29}$$

and

$$\sum_{j=1}^{m} W_j = \sum_{j=1}^{m} W_{j0} - \sum_{j=1}^{m} W_{j0}\alpha_j = W_0 - W_\infty - \sum_{j=1}^{m} W_{j0}\alpha_j \tag{30}$$

However, the global fractional decomposition of the solid is defined by eqn. (2), and

$$W = W_0 - (W_0 - W_\infty)\alpha \tag{31}$$

Because

$$W = \sum_{j=1}^{m} W_j + W_\infty \tag{32}$$

and taking into account eqns. (30) and (31)

$$\alpha = \frac{\sum_{j=1}^{m} W_{j0}\alpha_j}{W_0 - W_\infty} = \sum_{j=1}^{m} y_{j0}\alpha_j \tag{33}$$

where y_{j0} represents the initial mass fraction of component j, in a residue-free basis.

Differentiating eqn. (33) gives

$$\frac{d\alpha}{d\theta} = \sum_{j=1}^{m} y_{j_0} \frac{d\alpha_j}{d\theta} \tag{34}$$

The TG and DTG curves depend upon the various γ_j, β_j, kinetic functions and the composition of the solid mixture.

Simulations were carried out for an extensive range of values of the parameters, considering two reactive components, showing essentially three types of behaviour, as in the previous section.

Thus, when the reactivities are much different, there are two well separated rate peaks, each one corresponding to one reaction. The values of θ_m do not change with composition and, moreover, are practically the same as those obtained for the pure components. For instance, this is the case when $n_1 = 1$, $\gamma_1 = 30$, $\beta_1 = 10^7$, $n_2 = 1$, $\gamma_2 = 70$ and $\beta_2 = 10^{10}$. In this case, the DTG curves are exactly the same as those shown in Fig. 8 for these same reactions in series, if one takes $y_{1_0} = 1 - \mu$. This is so because the two reactions, when in series, occur in distinct temperature domains, i.e. for practical purposes, one occurs independently of the other.

When the reactivities of the two components become closer (e.g. $n_1 = 1$, $\gamma_1 = 10$, $\beta_1 = 10^2$, $n_2 = 1$, $\gamma_2 = 70$ and $\beta_2 = 10^{10}$), the peaks become partly superimposed, but in general the positions of the maxima do not change appreciably with the composition of the mixture. The curves are still very similar to those obtained with the same reactions in series (cf. Fig. 9), when accounting for the above mentioned relationship between parameters.

Finally, when the two components react in close domains of temperature (which is the case whenever the activation energies and pre-exponential factors are similar), there may be only one peak, the location of its maximum depending on the mass fraction of the components. The situation

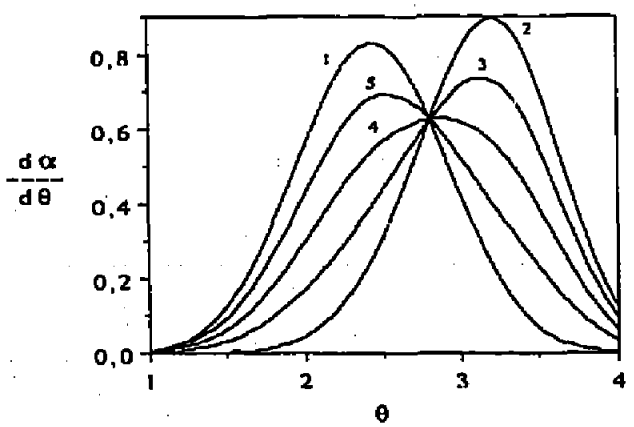

Fig. 11. DTG curves: two single reactions (1, $n_1 = 1$, $\gamma_1 = 10$, $\beta_1 = 10^2$; 2, $n_2 = 1$, $\gamma_2 = 20$, $\beta_2 = 10^3$); same reactions simultaneously (3, $y_{1_0} = 0.25$; 4, $y_{1_0} = 0.50$; 5, $y_{1_0} = 0.75$).

TABLE 5

Comparison between independent and consecutive reactions ($n_1 = 1$, $\gamma_1 = 10$, $\beta_1 = 10^2$, $n_2 = 1$, $\gamma_2 = 20$ and $\beta_2 = 10^3$)

Feature	y_{1_0} (independent reactions)			μ (consecutive reactions)		
	0.25	0.50	0.75	0.25	0.50	0.75
θ_m	3.13	2.86	2.53	2.53	3.11	3.24
$(d\alpha/d\theta)_m$	0.74	0.63	0.70	0.66	0.61	0.80

TABLE 6

Kinetic parameters (single reaction model) corresponding to the simulated thermograms with first order independent reactions ($\gamma_1 = 10$, $\beta_1 = 10^2$, $\gamma_2 = 20$ and $\beta_2 = 10^3$)

y_{1_0}	n	γ	β
0.25	0.75	10.6	41
0.50	0.85	9.7	39
0.75	0.95	9.5	49

is illustrated in Fig. 11. In this case, there are substantial differences with respect to the DTG curves for the same reactions in series shown in Fig. 10. Some features of these curves are shown in Table 5.

In order to illustrate the errors which may be involved when determining the kinetic parameters from curves of the type shown in Fig. 11 (assuming they result from a single reaction) the differential method of analysis was applied to the simulated results, considering a kinetic law of the type $f(\alpha) = (1 - \alpha)^n$.

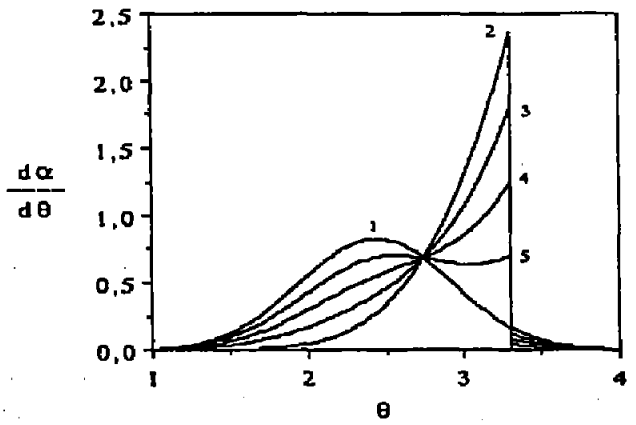

Fig. 12. DTG curves: two single reactions (1, $n_1 = 1$, $\gamma_1 = 10$, $\beta_1 = 10^2$; 2, $n_2 = 0$, $\gamma_2 = 20$, $\beta_2 = 10^3$); same reactions simultaneously (3, $y_{1_0} = 0.25$; 4, $y_{1_0} = 0.50$; 5, $y_{1_0} = 0.75$).

From eqn. (7)

$$\ln \frac{\frac{d\alpha}{d\theta}}{f(\alpha)} = \ln \beta - \frac{\gamma}{\theta} \quad (35)$$

The calculated parameters are shown in Table 6. It is observed that γ is quite close to the value corresponding to the faster reaction, but both β and the estimated reaction order are different from the values corresponding to any of the reactions.

DTG curves with only one relative maximum may also be obtained, even when the reaction orders are different, as exemplified in Fig. 12. Then, the necessary condition for this situation to occur is only that the two values of γ and the two values of β do not differ much one from the other. Figure 12 shows an interesting case (curve 5) where the rate remains practically constant over an extensive range of temperatures.

Application to the pyrolysis of lignocellulosic materials

Several authors have interpreted the pyrolysis of chemically complex materials such as coal [23–25] and wood [20] on the basis of a set of mutually independent reactions.

TABLE 7

Kinetic parameters for the first order reactions of the pseudo-components of chestnut wood and pine wood and respective mass fractions

Component	Mass fraction	E (kJ mol^{-1})	A (min^{-1})	y_0	γ	β
Pine wood						
1	0.20	83	4.2×10^{6}	0.25	34	2.5×10^{8}
2	0.53	146	1.2×10^{11}	0.65	60	7.0×10^{12}
3	0.02	77	2.6×10^{5}	0.025	32	1.5×10^{7}
4	0.03	60	1.7×10^{3}	0.04	25	1.0×10^{5}
5	0.02	139	3.0×10^{8}	0.025	57	1.8×10^{10}
6	0.01	130	1.9×10^{7}	0.01	53	1.1×10^{9}
Chestnut wood						
1	0.20	117	1.9×10^{10}	0.27	48	1.1×10^{12}
2	0.37	188	3.0×10^{15}	0.50	77	1.8×10^{17}
3	0.05	150	2.2×10^{11}	0.07	62	1.3×10^{13}
4	0.04	85	3.7×10^{5}	0.05	35	2.2×10^{7}
5	0.03	158	9.6×10^{9}	0.04	65	5.6×10^{11}
6	0.03	146	1.2×10^{8}	0.04	60	7.0×10^{9}
7	0.02	117	5.1×10^{5}	0.03	48	3.0×10^{7}

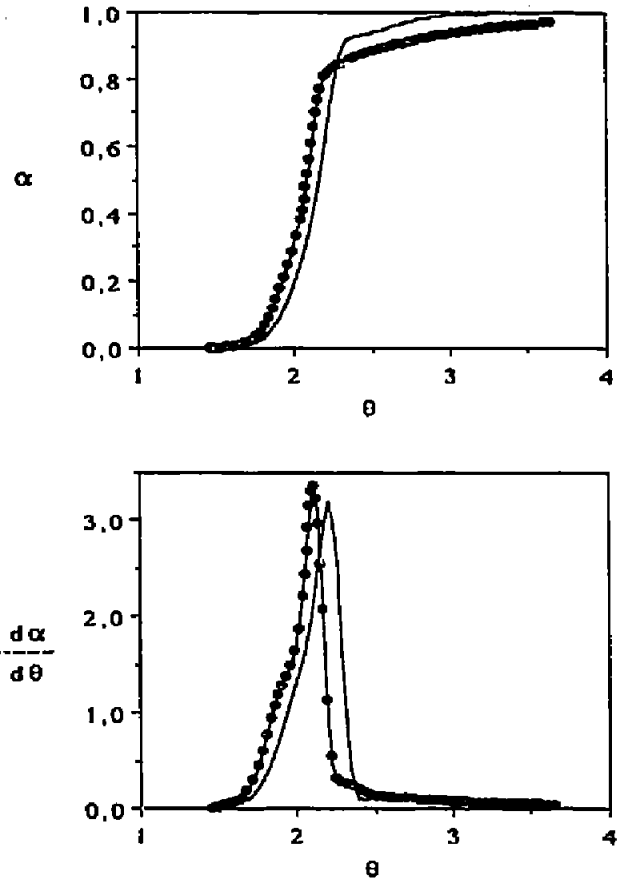

Fig. 13. TG and DTG experimental (●) and simulated (——) curves for the pyrolysis of pine wood ($b = 5\ \mathrm{K\ min^{-1}}$ and $T_0 = 293\ \mathrm{K}$).

Alves and Figueiredo [26] recently studied the kinetics of the pyrolysis of various lignocellulosic materials by multistage isothermal thermogravimetry, a technique which consists of recording the mass loss of the sample along successive isothermal steps of increasing temperature. A series of pseudo-components were identified in this way, each one reacting independently of the others with first order kinetics, and their mass fractions were estimated. Table 7 summarizes the results obtained for pine wood and chestnut wood, together with the dimensionless parameters used in the present context, taking $b = 5\ \mathrm{K\ min^{-1}}$ and $T_0 = 293\ \mathrm{K}$.

Dynamic thermogravimetric curves (TG, DTG) were simulated using these parameters and compared with the experimental curves obtained with a Mettler TA 4000 (M3TG/TG50) equipment (Figs. 13 and 14). The amount of sample used was ≈10 mg and the carrier gas was nitrogen (purity N46) with a flow rate of $200\ \mathrm{cm^3\ min^{-1}}$. A very reasonable fit is found in both cases, although there is a slight shift towards lower temperatures, then the predictions. This may result from some systematic error in temperature measurement in the earlier experimental set-up.

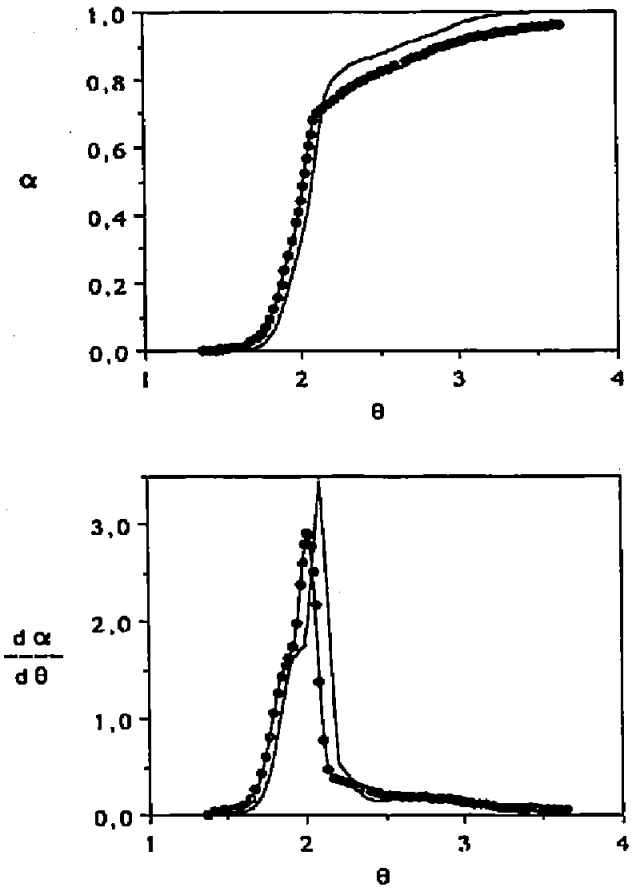

Fig. 14. TG and DTG experimental (●) and simulated (——) curves for the pyrolysis of chestnut wood ($b = 5\ \mathrm{K\ min^{-1}}$ and $T_0 = 293\ \mathrm{K}$).

ACKNOWLEDGEMENT

We are indebted to Mr. Luís M. Silva for performing the thermograms.

REFERENCES

1 J. Šesták, V. Satava and W.W. Wendlandt, Thermochim. Acta, 7 (1973) 333.
2 W.W. Wendlandt, Thermal Methods of Analysis, 3rd edn., Wiley, New York, 1986.
3 G. Pokol, S. Gál and E. Pungor, Thermochim. Acta, 105 (1986) 313.
4 M. Maciejewski and A. Reller, Thermochim. Acta, 110 (1987) 145.
5 K.N. Ninan, J. Therm. Anal., 35 (1989) 1267.
6 F.W. Wilburn, J.H. Sharp, D.M. Tinsley and R.M. McIntosh, J. Therm. Anal., 37 (1991) 2003.
7 J.H. Sharp, F.W. Wilburn and R.M. McIntosh, J. Therm. Anal., 37 (1991) 2021.
8 M. Reading, D. Dollimore and R. Whitehead, J. Therm. Anal., 37 (1991) 2165.
9 K.N. Ninan, Thermochim. Acta, 74 (1984) 143.
10 K.N. Ninan, Thermochim. Acta, 98 (1986) 221.
11 E. Koch, J. Therm. Anal., 33 (1988) 1259.
12 M.E. Brown, D. Dollimore and A.K. Galwey, in C.H. Bamford and C.F.H. Tipper (Eds.), Comprehensive Chemical Kinetics—Reactions in the Solid State, Vol. 22, Elsevier, Amsterdam, 1980.

13 H. Jüntgen and K.H. van Heek, Fortschr. Chem. Forsch., 13 (1970) 634.
14 H.E. Kissinger, Anal. Chem., 29 (1957) 1702.
15 J.G. McCarty, P.Y. Hou, D. Sheridan and H. Wise, in L.F. Albright and R.T.K. Baker (Eds.), Coke Formation on Metal Surfaces, Am. Chem. Soc. Symp. Series, Vol. 202, American Chemical Society, Washington DC, 1982, p. 253.
16 J.L. Figueiredo and J.J.M. Órfão, Catal. Today, 5 (1989) 385.
17 N.S. Figoli, J.N. Beltramini, E.E. Martinelli, M.R. Sad and J.M. Parera, Appl. Catal., 5 (1983) 19.
18 J.H. Flynn, Thermochim. Acta, 37 (1980) 225.
19 J.H. Flynn and L.A. Wall, J. Res. Natl. Bur. Stand., 70A (1966) 487.
20 F. Shafizadeh, J. Anal. Appl. Pyrol. 3 (1982) 283.
21 S.S. Alves and J.L. Figueiredo, J. Anal. Appl. Pyrol. 17 (1989) 37.
22 S.M. Ward and J. Braslaw, Combust. Flame, 61 (1985) 261.
23 D.E. Anthony and J.B. Howard, AIChE J., 22 (1976) 625.
24 J.P. Elder, J. Therm. Anal., 29 (1984) 1327.
25 T. Coll, J.F. Perales, J. Arnaldos and J. Casal, Thermochim. Acta, 196 (1992) 53.
26 S.S. Alves and J.L. Figueiredo, J. Anal. Appl. Pyrol., 13 (1988) 123.